Materials Science & Engineering B 231 (2018) 11–17

Contents lists available at ScienceDirect

Materials Science & Engineering B

journal homepage: www.elsevier.com/locate/mseb

CNTs' array growth using the floating catalyst-CVD method over different substrates and varying hydrogen supply

O. Guellati[a,b,c,*], D. Bégin[b], F. Antoni[e], S. Moldovan[d], M. Guerioune[a], C. Pham-Huu[b], I. Janowska[b,*]

[a] Laboratoire d'Etude et de Recherche des Etats Condensés (LEREC), Département de Physique, Université Badji-Mokhtar de Annaba, BP. 12, Annaba 23000, Algeria
[b] Institut de Chimie et Procédés pour l'Energie, l'Environnement et la Santé (ICPEES) – ECPM – CNRS – UMR 7515 Université de Strasbourg, 25 rue Becquerel, 67087 Strasbourg Cedex 2, France
[c] Université de Souk-Ahras, BP. 1553, Souk-Ahras, 41000, Algeria
[d] Institut de Physique et Chimie des Matériaux de Strasbourg (IPCMS), UMR 7504 du CNRS, Université de Strasbourg, France
[e] Laboratoire ICube – DESSP (UMR7357 CNRS, Université de Strasbourg), 23 Rue du Loess – BP20, 67037 Strasbourg Cedex 02, France

ARTICLE INFO

Keywords:
Aligned CNTs
Sapphire substrate
Floated-catalyst
CVD
H_2 etching

ABSTRACT

In the present investigation, we point out the effect of the substrate crystallinity on the growth rate, efficiency, quality and the structure of synthesized aligned carbon nanotubes (CNTs). Three substrates are tested: amorphous alumina (Al_2O_3), silica (Si/SiO_2), and crystalline alumina (sapphire). The growth is carried out using the floating catalyst-CVD process with the ferrocene-toluene solution as precursor. In addition, different concentrations of H_2 in the gas supply are investigated. It is observed that the sapphire substrate provides a more homogenous forest of vertically oriented straight nanotubes with small diameter, despite initial horizontal alignment of the nanotubes. In the presence of H_2, long arrays of high L/Φ aspect ratio nanotubes were obtained with a reduction of diameter and the number of walls. L/Φ aspect ratio in the case of 7% H_2 is c.a. 3600 for sapphire substrate, 1500 and 2000 for alumina and silica amorphous substrate, respectively. When sapphire substrate is used, the increase of H_2 to 15% provides the L/Φ aspect ratio of ~14,000.

1. Introduction

The efficient exploitation of CNT properties, such as mechanical, electrical or surface area is often requiring alignment of the tubes. The alignment of high density CNTs to a required direction are under investigation for a wide range of practical nanotechnology applications, such as high performance electronic and optoelectronic nano-devices such as CNT based field-emission devices, transistors, diodes and resistors, electrochemical energy storage devices like CNT supercapacitors, gas sensors, heterogeneous catalysis, hydrogen storage, … [1–3]. More research efforts are required however to control not only their direction but also the structural quality of the arrays and nanotubes themselves as advanced solid-state materials.

Two classes of alignment techniques can be distinguished from growing the tubes along a given direction, either horizontal or vertical depending on the substrate crystallinity [4–7]. To control them, it is important to understand their nucleation and their growth processes. The CNT-CNT or the CNT-substrate interactions, in addition to the arrangement and activity of the catalytic sites, determine the CNTs grow in an isolated, tangled or aligned configuration [8–10]. Moreover, the strong influence of atomic arrangement of surface such as sapphire is suggested not only to influence the growth direction but also the tubes chirality [11,12]. In the case of catalyst deposited on the substrate before the growth of CNTs is initiated, the alignment is only horizontal to the substrate. In turn, generally, at higher catalyst density and CNT growth rate, a vertically aligned "VA" growth mode is favourable; the CNTs self-orient perpendicularly to the substrate due to an initial crowding and continue to grow upward in this direction [10,13].

In contrast to previous synthesis method, floating catalyst CVD is promising for in-situ nucleation and growth as one step efficient method, but also quite versatile for scale-up production of selective CNTs [14]. Depending on different processes and growth system designs, the growth rates of CNTs using this method can be limited by basic parameters such as substrate features, substrate-catalyst contact energy, catalyst poisoning and hydrocarbon precursors, … [4,15,16]. There are a number of reports on production of CNTs based on continuous CVD route discussing either the experimental [14–24] or theoretical [25–30] factors of the process. Besides these, the kinetic aspects

* Corresponding authors at: Laboratoire d'Etude et de Recherche des Etats Condensés (LEREC), Département de Physique, Université Badji-Mokhtar de Annaba, BP. 12, Annaba 23000, Algeria (O. Guellati).
E-mail addresses: ouanassa.guellati@univ-annaba.org (O. Guellati), janowskai@unistra.fr (I. Janowska).

https://doi.org/10.1016/j.mseb.2018.03.001
Received 16 August 2017; Received in revised form 18 December 2017; Accepted 20 March 2018

such as local reaction rates at the catalyst surface, diffusion of precursor to the catalyst through as grown CNTs and catalytic surface poisoning by other formed carbonaceous species are actually the subject of important studies [17,31]. Mainly, the role of H_2 has been described quite extensively in both the vapour grown carbon fibres and the carbon nanotubes literature. H_2 is known to have the ability to either accelerate or suppress the formation of carbon [26,27]. It has also been shown for this type of process that H_2 can also plays an important role in the control of the CNTs diameter as reported in our previous work by studying the synergetic effect of EtOH/hydrogen on the growth rate of VA-MWNTs [17], brakes the deposited catalyst layer into smaller particles [16] as well as helps to prevent the formation of amorphous carbon impurities [18,19]. The H_2 concentration should be however low enough to avoid excessive surface carbon removal by the formation of CH_4, which would lead to a formation of lower CNT yield [31].

The organisation of CNTs into horizontally and vertically aligned arrays on surfaces, which continues to be a major challenge in controlled production of macroscopically CNTs, has been significantly advanced by the development of directional flow or substrate domain [16,18]. More recently [19–21], aligned growth by epitaxial orientation on well defined crystal surfaces, directed by atomic steps, nanofaces or atomic rows or by applied electrical field, has opened up new ways of organizing CNTs on surfaces into perfectly aligned arrays.

Ago's group have proposed, lately, a new method based on atomic arrangement as guide and specific crystallographic growth direction [5,6,8,11,19]. They tried to understand the role of catalyst-surface interactions onto different substrates such as sapphire, basing, on their surface energy that affects the surface diffusion length, the catalyst particle size and the CNTs density. In addition, the difference between base or tip growth mechanism is often explained in terms of adhesion force strong or weak adhesion, respectively between the catalyst particle and the substrate. An important effect of Al_2O_3 substrate was found on the production of highly dense and nanosized Co particles, owing to a low surface diffusivity, and reduced agglomeration of metal atoms [10].

In this investigation, we show a study on the influence of the substrate crystallinity on the growth and the morphology of macroscopic CNTs obtained with floating-catalyst CVD process, assisted or not by H_2. In this regard, the CVD process with ferrocene dissolved in toluene ($FeCp_2$-toluene) as floated catalyst has been conducted on crystallinized sapphire wafers and amorphous alumina. Additionally, the Si/SiO_2 wafers were tested in the same conditions. The effect of H_2 concentration (0, 7 and 15 vol%) in Ar flow on the MWNTs alignment selectivity, density and crystallinity of the formed arrays and nanotubes themselves have been investigated as well.

2. Experimental section

2.1. Synthesis of aligned carbon nanotubes "VACNTs"

All samples were prepared by a floated-catalyst CVD (Fig. 1) by injection of a constant concentration of the ferrocene "$FeCp_2$"-toluene (20 g/L) with a constant flow rate of carrier gas (Argon "Ar", 1.5 L/min) and with hydrogen "H_2" gas addition (7 and 15 vol% of Ar or 0 vol%). So, the total gas supply will be 1.5 L/min Ar + 0.105 L/min H_2 = 1.6 L/min.

In these conditions, a total amount of 20 mL of the $FeCp_2$-toluene solution is injected continuously with the flow rate of 0.33 mL/min into the heated reactor using a programmable syringe system.

The substrates used for the oriented growth of the arrays using floated CCVD are: silicon wafers (Siltronix, Si_{100}, 10 × 10 mm^2 with 525 μm thickness) thermally oxidized to obtain SiO_2 barrier layer of 100 nm thickness, alumina wafers (Crystal, 20 × 10 mm^2 with 0.45 mm thickness) and r-plane sapphire wafers (Crystal, one side polished, [1–102] 15 × 15 mm^2 with 0.45 mm thickness).

In general, the process starts by the evacuation of the air from quartz reactor using Ar flow for 30 min followed by heating the reactor to 870 °C. The temperature is maintained for one hour at atmospheric pressure. Then the solution of Fe-Cp_2-toluene/Ar (and H_2) is injected for CNT array growth. After the synthesis, the reactor is cooled down under Ar flow. According to eye- observations and FESEM analysis, the CNTs growth are carpet (« sheet ») geometry (see Fig. 1b).

After that, the CNT arrays are purified in order to remove the remaining iron catalyst from the samples by acid treatment step using aqua regia (HCl: HNO_3 = 1:3) at 80 °C under stirring during 2 h, then, washed and dried at 80 °C for all the night. The volume density of products was then calculated by dividing the deposit mass by the substrate volume.

2.2. Characterization techniques

JEOL 6700-FEG microscope field emission scanning electron microscope (FESEM) accompanied with Energy Dispersive X-ray spectroscopy (EDX) quantitative analysis was employed to examine the morphology and the purity of products: the length, the orientation and the density estimation were obtained from cross-sectional images of the samples.

JEOL 2100F high and low magnification transmission electron microscopy (TEM) working under an accelerated voltage of 200 kV was carried out with a point-to-point resolution of 0.23 nm in order to characterize the grown CNT microstructure. A drop of dispersed CNTs in ethanol medium was deposited onto a holey carbon coated copper TEM grid for examination.

Tristar Micromeritics sorptometer using nitrogen as adsorbant at liquid nitrogen temperature was used to specific surface area measurements. Before measurements, the sample was outgassed at 250 °C for 3 h minimum in order to desorb impurities and moisture.

Setaram apparatus Thermo-Gravimetry Analysis (TGA) was carried out under air flow (20 mL/min) where the experiments were performed from ambient to 1000 °C with a heating rate of 10 °C/min.

Microraman RENISHAW spectrometer (RAMASCOPE 2000 coupled to an optical microscope with a spot size of 1 μm^2 and 1 cm^{-1} resolution) operated with a He-Ne Laser beam excitation of 632.8 nm wavelength was employed to perform Raman spectroscopy. The D/G peak areas ratio was used for the determination of the defective (~1350 cm^{-1}) to graphitic (~1589 cm^{-1}) carbon ratio present inside the as-synthesized CNT arrays.

3. Results

It is already well established in the literature that the CNT grown on the sapphire substrates are horizontally aligned in the case of the predeposited catalyst due to their interaction with atomically arranged substrate surface [17]. Indeed, in the present investigation, i.e. when floated catalyst is provided in continuous way, the horizontal arrangement is observed on sapphire substrate for the first growth period, while next it changes gradually to vertical orientation. In contrast, the growth on amorphous substrates i.e. silica and alumina wafers (same for quartz reactor walls), the MWNTs are oriented perpendicular to substrate from the beginning as generally observed by researcher using amorphous substrate with same CVD approach [32,33].

In Table 1, the weight, thickness and density of obtained CNT arrays are presented as well as the diameter of the tubes, for different supports and percentage of H_2. These results correspond to the crude CNT arrays without purification step. According to the obtained results reported in Table 1, the MWNT volume density depends slightly on the substrate nature and changes in general with the H_2 concentration in the carrier gas during the growth, especially in the case of sapphire substrate.

The addition of hydrogen decreases the deposited carbon weight and the growth rate for a given substrate due to the carbon etching action, except the sapphire with 15% of H_2. In the latter case despite the low volume density and reduced tubes diameter, the height of tubes

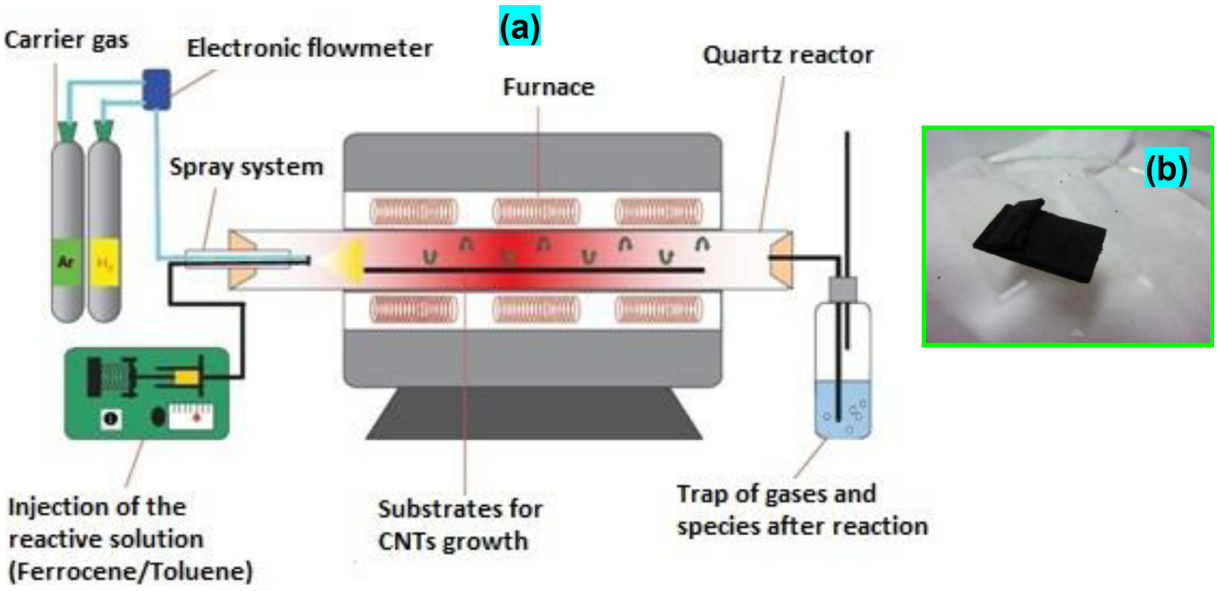

Fig. 1. (a) Schema of floated CCVD process. (b) Photos of the SiO_2/Si substrate after growth of CNTs forest.

Table 1
Effect of H_2/Ar ratio and substrate crystallinity on yield, density and thickness of CNT arrays as well as tubes diameter.

Substrate	H_2/Ar (vol.%)	Deposited mass (mg)	ρ_V[(a)] (g/cm^3)	Fe[(b)] (wt.%)	Φ[(c)] (nm)	Thickness (μm)	Growth rate (μm/min)
Si/SiO_2	0	38,2	0,27	3	25–45	542	9
	7	0,3	0,07	11	20–35	22	0,4
	15	1,3	0,28	17	35–60	18	0,3
Al_2O_3	0	7,9	0,25	–	35–50	211	3,5
	7	5,6	0,22	–	45–75	129	2,2
	15	4,1	0,19	–	30–50	109	1,8
r-Sapphire	0	6,3	0,18	22	15–25	155	2,6
	7	4,2	0,21	21	15–30	91	1,5
	15	4,1	0,09	24	10–20	213	3,6

[(a)] Volume density of deposited CNT from weight versus wafer volume.
[(b)] Residual catalyst weight percentage after TGA analysis for crude VACNTs.
[(c)] Diameter range of most MWNTs obtained from FESEM micrograph histograms.

array is significantly improved. This is linked to a relatively high grown rate of the tubes, which contrary to the amorphous substrates, increases with H_2 concentration. The presented density values are however estimated since they are based on the substrate- free CNTs weigh. The product includes the carbon and iron catalyst remaining from the synthesis with variable percentage. Moreover, H_2 eliminates the amorphous carbon deposited on the surface of catalyst during the growth of CNTs. This phenomenon is well known in the literature, the excess of carbon supply makes it fast decomposition into amorphous carbon on the catalyst surface and inhibits the catalyst action (poisoning of the catalyst).

The FESEM micrographs presented for the samples obtained with 7% H_2 in the gas supply clearly show straight, pure and well aligned CNTs grown on the sapphire substrate (Fig. 2c, d and g). This is not the case of the growth over the amorphous substrates (SiO_2 – Fig. 2a and Al_2O_3 – Fig. 2b) where a less dense alignment with secondary NTs random branches on the pre-deposited tubes surface can be clearly observed (Fig. 2e and f, respectively). Such high density CNT growth on crystalline sapphire substrate, as illustrated here in FESEM micrographs, can be explained by the deposition of small and high density catalyst particles promoted by the use of ordered area substrate and related interactions between catalyst and substrate surface. In addition, concerning the sapphire substrate, an initial alignment direction of the grown tubes is horizontal then the direction changes gradually to vertical one.

This shows that the impact of atomic arranged substrate and its interactions with grown carbon is weakened with time by the interactions between the tubes and related continuous supply of the catalyst. The low magnification FESEM micrographs demonstrate that the CNT array height on sapphire is uniform and reaches for 7% H_2, about 90 μm (Fig. 2c). With amorphous substrate, random alignment and height of about 20 μm and 130 μm for SiO_2 and Al_2O_3 are achieved respectively.

The difference in term of homogeneity of the obtained tubes and their alignments over amorphous and crystalline substrates is well observed at the top of the arrays (Fig. 2a-d, and insets). Considering the base-growth type of the arrays, their tops observed by SEM includes the tubes grown at the beginning of the process. Smooth, almost flat and homogenous top is seen for sapphire grown tubes, while highly entangled, inhomogeneous and rough top present the tubes grown over amorphous substrate.

The mechanism of the aligned CNTs arrays growth is not the goal of this work. According to the literature data, the base-growth and the related strong interactions between the catalysts and the substrates were previously observed for silica and alumina substrates [34–36]. However, it was also found that the mechanism can be changed by modifying the oxidation state of the catalyst and so the investigation of

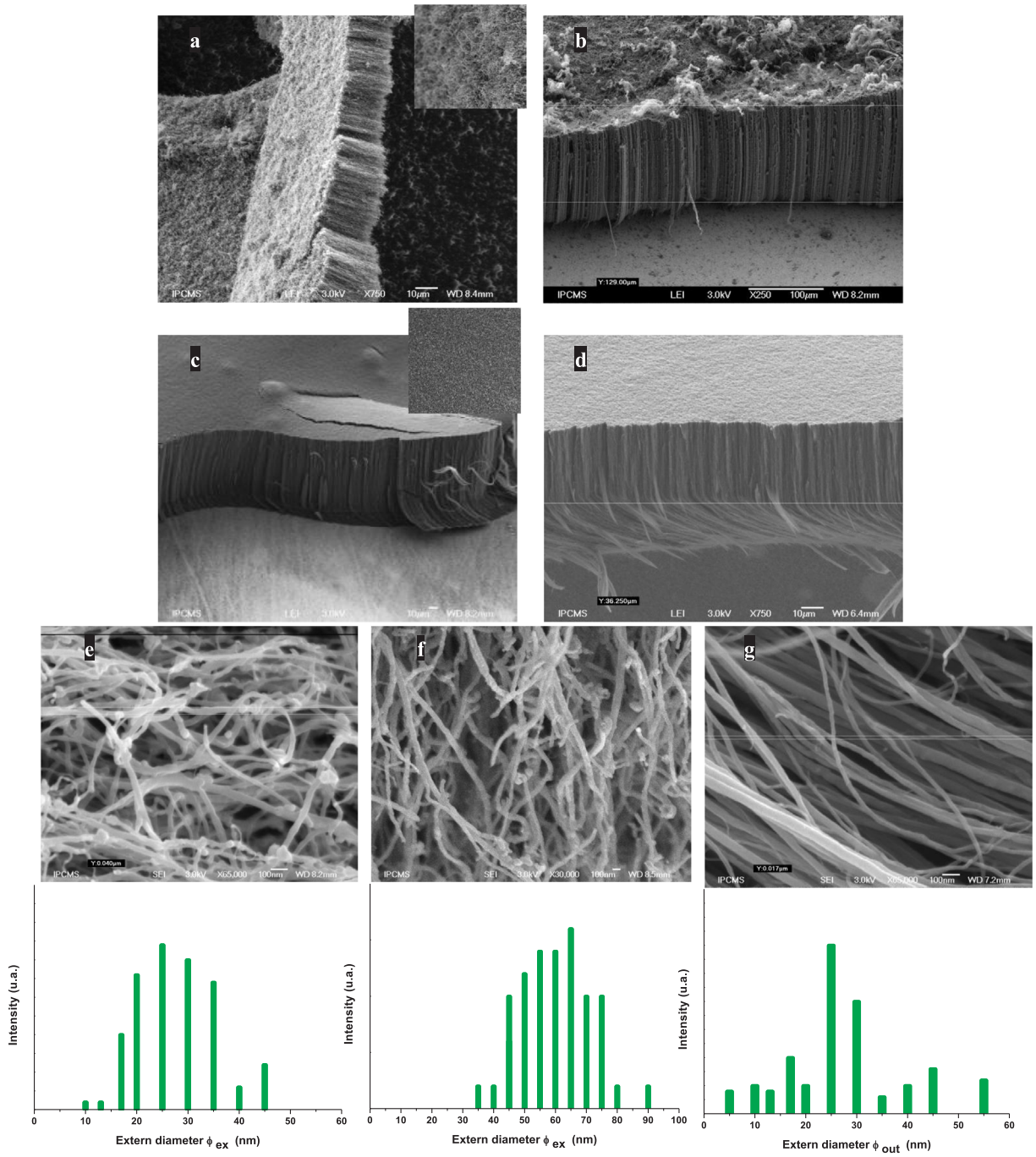

Fig. 2. FESEM micrographs of aligned CNTs synthesized on three kinds of substrate with 7 vol% H_2 at 870 °C for 1 h: non crystalline substrate "(a, e) Si/SiO_2 and (b, f) Al_2O_3" and crystalline one, sapphire "(c, g, d).

the mechanism should be undertaken individually for the growth with varying synthesis conditions (supplied gases, substrates and temperatures).

We proved however through the bi-oriented growth that the growth direction is programmed by substrate surface structure; the phenomena reported by Ago's group as « atomic arrangement programmed growth ». The initial horizontal alignment is then explained by anisotropic Van der Waals interactions between CNTs and the crystalline surface with anisotropic atomic arrangement of the single crystal planes in agreement with reported results in the literature [29,30]. It is possible that at lower catalyst density and synthesis duration the horizontal or inclined arrays would be obtained. We do not investigate the change of alignment direction in term of growth duration since we do not know how the rate of this growth changes with time. The alignment direction changes however gradually with the continuously increasing catalysts density, what overcomes the interactions of tubes with the substrate.

Fig. 3a and b show representative TEM micrographs of MWNTs with few walls (9 and 4) and with an external diameter of about 15 nm and 10 nm, in the case of silica and sapphire, respectively. The impurities present in the raw products were just thin layer of amorphous carbon on the NTs surface as shown in HRTEM micrographs and some encapsulated iron based particles, next removed by chemical purification by oxidative acid treatment.

The average bulk density of the samples obtained without H_2 is of 0.27 g/cm^3 and 0.25 g/cm^3 for amorphous substrates and 0.18 g/cm^3 for crystalline one, which is very close to the results obtained in

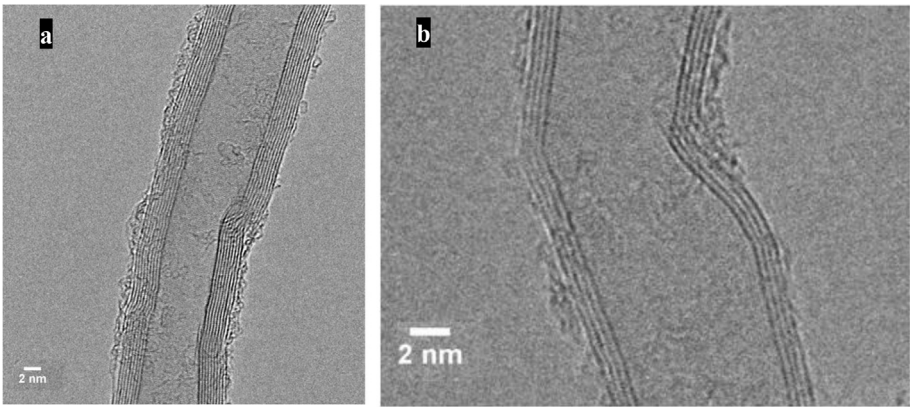

Fig. 3. High resolution TEM micrographs of CNTs obtained with 7 vol% H_2 on (a) silica and (b) sapphire wafers.

reference [28]. As mentioned already above, the introduction of H_2 (even small amounts, 7 vol%) reduces the deposition of carbon and apart from lowered density, the variation in CNT diameter is observed. In the case of sapphire substrate the diameter is significantly reduced and this reduction with H_2 concentration increases is more pronounced that for amorphous substrates. In general, ferrocene decomposes into Fe, H_2, CH_4, C_5H_6 and other hydrocarbons at temperature superior than 500 °C [37]. So, the presence of produces from this H_2 decomposition is not sufficient to change the structure of CNTs in the significant manner.

Fig. 4 illustrates the FESEM micrographs showing the general morphology of MWNT arrays obtained on sapphire with different concentration of H_2 in Ar gas supply. It correlates the MWNTs length and diameters with the H_2/Ar ratio percentage. The higher magnification reveals a clear lowering of the average diameter as the H_2 concentration increases, with relatively narrow diameters distribution (histograms Fig. 4).

It seems also that H_2 plays most prominent role in the case of sapphire, where not only reduced diameter but also length of tubes is strongly enhanced resulting into high aspect ratio tubes (L/Φ) of about 3600 for sapphire substrate, 1500 and 2000 for alumina and silica amorphous substrate, respectively) in the case of 7% H_2 and lowered walls number as revealed by followed TEM analysis. In the case of sapphire, with increasing H_2 to 15%, we found L/Φ aspect ratio of about 14,000.

Fig. 5 displays representative TEM micrographs of synthesized MWNTs with 0 vol% H_2 and 15 vol% H_2 for both amorphous silica and crystalline sapphire substrates. A reduction of the external diameter as well as the number of the walls in the produced tubes can be clearly observed with H_2 increase. For example, we can see the reduction of the MWNT outer diameters, from an average of 25 nm to 8 nm and corresponding to a change in the number of walls from 11 to 6 for 0 vol% and 15 vol%, respectively. Such modification of MWNT morphology is in agreement with earlier reports for MWNTs grown by a CVD system with a pre-deposited catalyst [16,18,19]. It is worthy to note that the reduction of the number of walls is simultaneously related here to the diminished external diameter, since there is no visible change of internal tube diameter.

According to the thermo-gravimetric analysis presented by the first derivative in Fig. 6, aligned-MWNTs on sapphire show narrow peaks and are stable up to almost 600 °C. The combustion temperature is

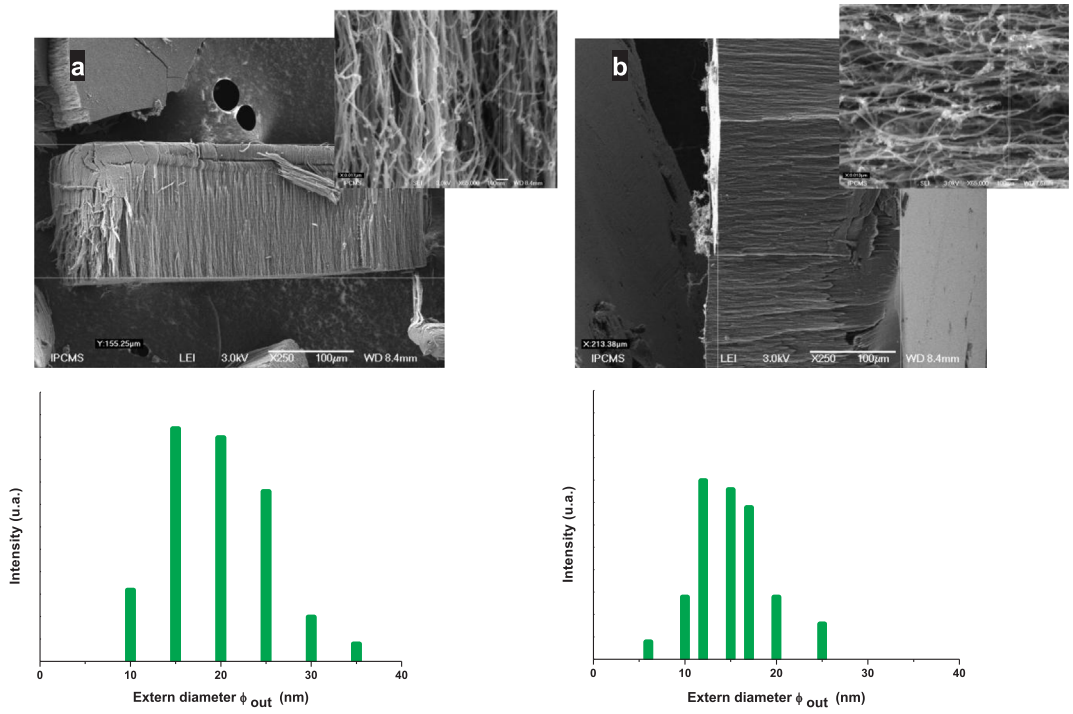

Fig. 4. FESEM micrographs of the aligned CNTs obtained over sapphire substrate as a function of H_2 percentage and the tubes histograms: 0 vol% (a) – 15 vol% (b).

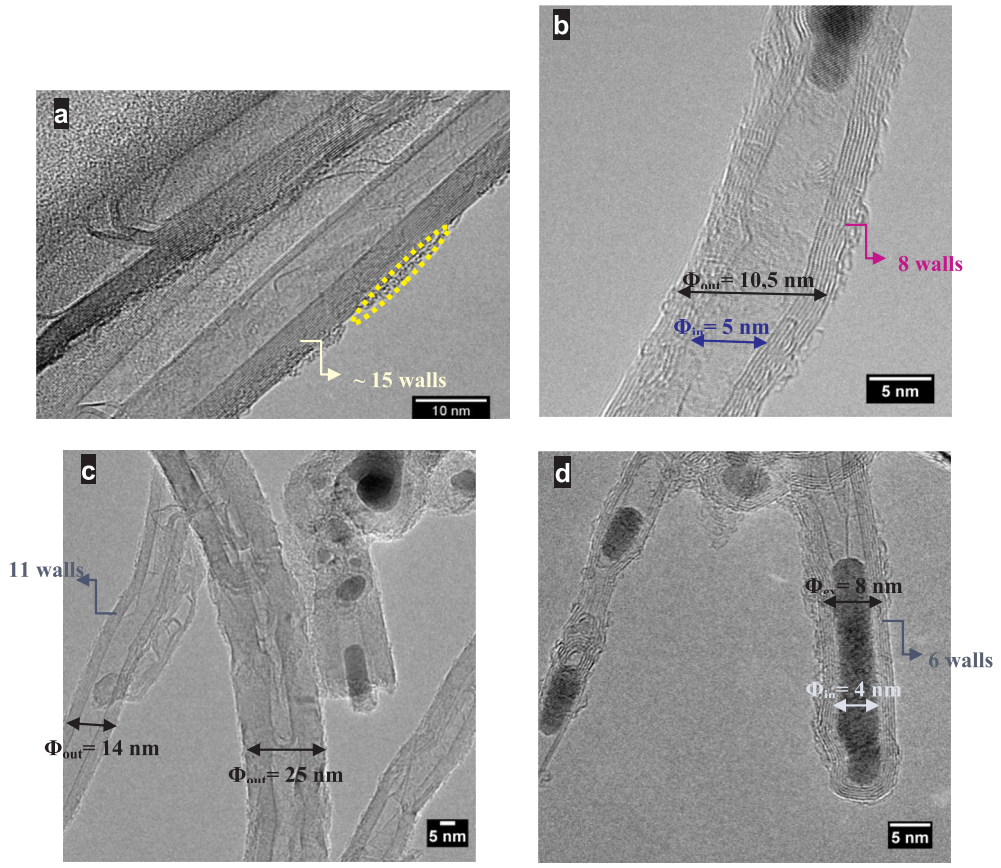

Fig. 5. Representative TEM micrographs of the crude aligned MWNTs on silicon (top) and sapphire wafers (down) with different H_2 percentage: (a, c) 0 vol% and (b, d) 15 vol%.

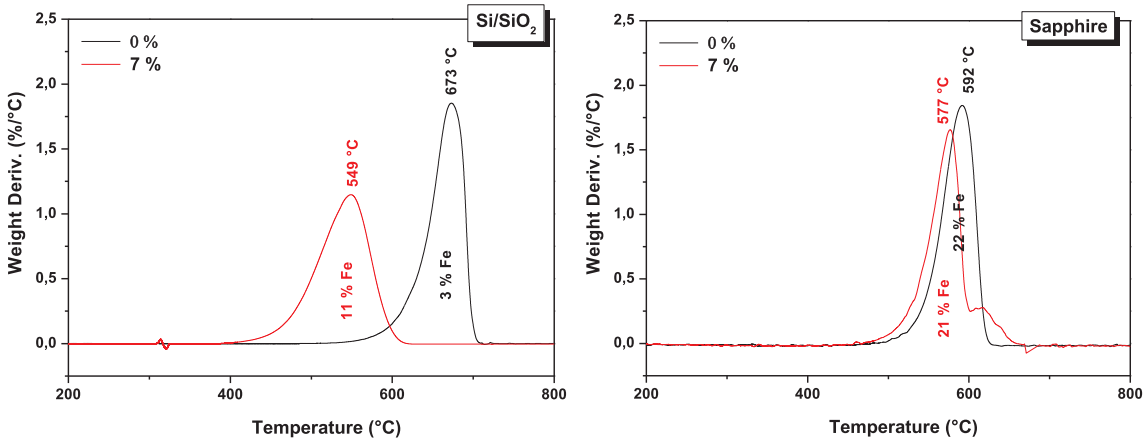

Fig. 6. H_2 percentage effect on an oxidative behavior through thermal analysis of the crude aligned MWNTs synthesized over amorphous and crystalline substrates.

slightly lower than for SiO_2 substrate. The important decrease in the combustion temperature in the case of 7% H_2 is related to much higher amount of remaining iron-based catalyst. During the TGA analysis, the remaining iron, which is in fact the iron oxide species, acts as oxidation catalyst and start to oxidised (burn) the carbon sample at much lower temperature. Consequently, the influence of the remaining catalyst can be clearly seen for silica wafer, where drastic decrease of the combustion temperature takes place for 7% H_2 compared to 0% H_2 due to the enhanced iron content, iron which is well known as a combustion catalyst of carbonaceous materials. The excess of the catalysts found in the samples grown over crystalline sapphire substrate have been particularly observed inside the tubes, as illustrated in Fig. 5. The following chemical purification allowed removing most of this residual catalyst down to about 3 wt%.

The specific surface area for SiO_2 and sapphire substrate grown CNTs have been measured by N_2 adsorption and is around 56 m^2/g and 66 m^2/g, respectively, which is in agreement with the fact that the tube diameter over sapphire is lower.

Raman spectra performed for MWNTs obtained on the two substrates are shown in Fig. 7. There are several factors that influence Raman spectra G bands (associated with graphitic carbon) and D bands (associated with lattice defects) [23–25]. Both peaks are shifted towards higher wavenumber in the case of sapphire substrate (3 cm^{-1}).

The Raman spectra show also a low ratio between the D and G relative area confirming the low amorphous carbon content and structural defects for the two substrates, as reported in Fig. 6c. The A_D/A_G is indeed a purity/crystallinity index to assess the quality of produced MWNTs [25], used as well earlier for the floated catalyst CVD process

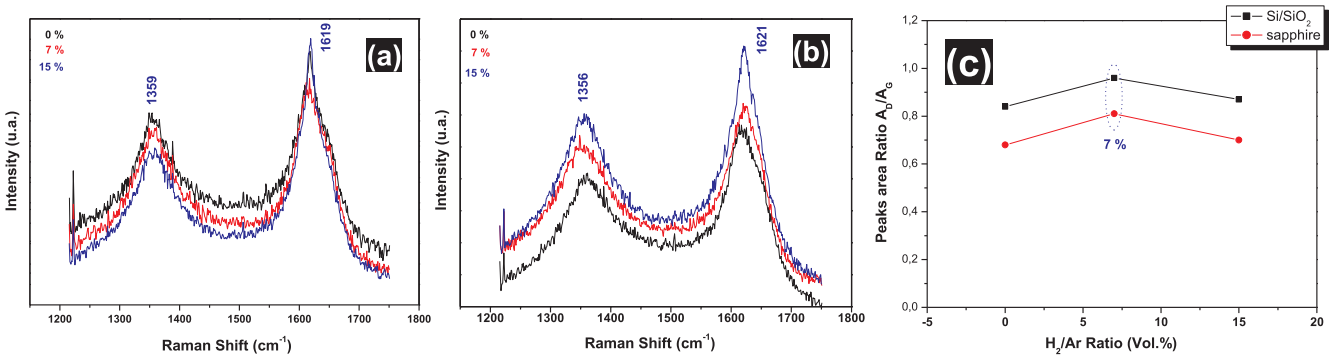

Fig. 7. Raman spectra recorded with the H_2/Ar ratio evolution for silicon (a) and sapphire (b) wafers, respectively. (c) Their D/G peaks area ratio as a function of the H_2 percentage in Ar flow.

obtained tubes [17,38]. Their values are in the range of 0.8–0.95 and of 0.65–0.85 for SiO_2 and sapphire, respectively.

Finally, the production of higher density CNTs due to the continuously injected catalysts and generally easy modified by changing the concentration of the injected solution. The yield of such produced CNTs is also much higher than in the case of the pre-deposited catalyst. So, the selectivity of CNTs deposition is however much lower. The tubes growth also around the given substrate, i.e. on the reactor walls which are quartz (SiO_2) made and where strong interactions between the walls and iron based catalysts occur. Depends on the envisaged applications, the pre-deposited (growth only over the substrate) or floated catalysts can be then preferable.

4. Conclusion

In this work, we have observed the influence of substrate crystallinity (amorphous "SiO_2 and Al_2O_3" and single crystalline r-plane sapphire) on the morphology of aligned-MWNT arrays synthesized using floated catalyst CVD process, in the presence or not of hydrogen.

The results show that the initial alignment takes place horizontally to the sapphire substrate and it changes after some time for vertical direction. The use of crystalline sapphire substrate permits to obtain the arrays of homogenous, straight tubes with lowered diameter and number walls (few layer walls), and once coupled with significant hydrogen content (15%), the long, thin tubes with high aspect ratio are achieved.

We show that not only the orientation, but also the density and the alignment are affected by the crystal plane of the sapphire substrate and its effect is still enhanced when assisted by carbon etching hydrogen. Consequently, the self-organized alignment method produced very dense, well aligned and height MWNT networks without any requirement of special technique or equipment.

Acknowledgements

The present work was partially supported by the doctoral scholarship grant of the Algerian Ministry of Higher Education and Scientific Research. The authors would like to acknowledge M. Th. Romero (ICPEES) for performing FESEM experiments.

References

[1] K. Iakoubovskii, Cent. Eur. J. Phys. 7 (4) (2009) 645–653.
[2] L. Truong-Phuoc, T. Truong-Huua, B. Lam Nguyen-Dinh, W. Baaziz, T. Romero, D. Edouard, D. Begin, I. Janowska, C. Pham-Huu, Appl. Catal. A: General. 469 (2014) 81–88.
[3] P. Serp, M. Corrias, P. Kalck, Appl. Catal. A: General. 253 (2) (2003) 337–358.
[4] M.C. Schnitzler, A.J.G. Zarbin, J. Nanopart. Res. 10 (4) (2008) 585–597.
[5] H. Ago, Y. Nakamura, Y. Ogawa, M. Tsuji, Carbon 49 (1) (2011) 176–186.
[6] H. Ago, N. Uehara, K.-I. Ikeda, R. Ohdo, K. Nakamura, M. Tsuji, Chem. Phys. Lett. 421 (4–6) (2006) 399–403.
[7] S. Handuja, P. Srivastava, V.D. Vankar, Nanoscale Res. Lett. 5 (2010) 1211–1216.
[8] H. Ago, I. Tanaka, M. Tsuji, K.-I. Ikeda, S. Mizuno, J. Phys. Chem. C. 112 (47) (2008) 18350–18354.
[9] C. Pint, S. Pheasant, N. Nicholas, C. Horton, R. Hauge, J. Nanosci. Nanotech. 8 (11) (2008) 6158–6164.
[10] H. Ohno, D. Takagi, K. Yamada, S. Chiashi, A. Tokura, Y. Homma, Japan J. App. Phys. 47 (4) (2008) 1956–1960.
[11] H. Ago, K. Imamoto, T. Nishi, M. Tsuji, T. Ikuta, K. Takahashi, M. Fukui, J. Phys. Chem. C. 113 (30) (2009) 13121–13124.
[12] N. Ishigami, H. Ago, K. Imamoto, M. Tsuji, K. Iakoubovskii, N. Minami, J. Am. Chem. Soc. 130 (30) (2008) 9918–9924.
[13] I. Janowska, S. Hajiesmaili, D. Bégin, V. Keller, N. Keller, M.J. Ledoux, C. Pham-Huu, Catal. Today 145 (2009) 76–84.
[14] A. Gohier, C.P. Ewels, T.M. Minea, M.A. Djouadi, Carbon 46 (10) (2008) 1331–1338.
[15] R. Kamalakaran, M. Terrones, T. Seeger, Ph. Kohler-Redlich, M. Rühle, Y.A. Kim, T. Hayashi, M. Endo, App. Phys. Lett. 77 (21) (2000) 3385–3387.
[16] M. Maret, B. Saubat, J. Flock, A. Mantoux, F. Charlot, D. Makarov, Chem. Phys. Lett. 495 (1–3) (2010) 96–101.
[17] O. Guellati, I. Janowska, D. Bégin, M. Guerioune, Z. Mekhalif, J. Delhalle, S. Moldovan, O. Ersen, C. Pham-Huu, App. Catal., A 423–424 (2012) 7–14.
[18] M. Maret, K. Hostache, M.-C. Schouler, B. Marcus, F. Roussel-Dherbey, M. Albrecht, P. Gadelle, Carbon 45 (1) (2007) 180–187.
[19] H. Ago, N. Ishigami, K. Imamoto, T. Suzuki, K.-I. Ikeda, M. Tsuji, T. Ikuta, K. Takahashi, J. Nanosci. Nanotech. 8 (11) (2008) 6165–6169.
[20] N. Yoshihara, H. Ago, K. Imamoto, M. Tsuji, T. Ikuta, K. Takahashi, J. Phys. Chem. C 113 (19) (2009) 8030–8034.
[21] H. Ago, et al., Appl. Phys. Lett. 90 (2007) 3 123112.
[22] O. Guellati, S. Detriche, M. Guerioune, Z. Mekhalif, J. Delhalle, Int. J. Nanoelectr. Mater. 3 (2010) 123–131.
[23] A.C. Ferrari, J. Robertson, Phys. Rev. B. 61 (2000) 14095–14107.
[24] R. Saito, A. Gruneis, G.G. Samsonidze, V.W. Brar, G. Dresselhaus, M.S. Dresselhaus, A. Jorio, L.G. Cancado, C. Fantini, M.A. Pimenta, A.G. Souza Filho, New J. Phys. 5 (2003) 157.1–157.15.
[25] H.M. Heise, et al., J. Raman Spectrosc. 42 (2011) 294–302.
[26] H. Wang, S. Zhang, S.E. Ong, J. Guo, Nanosci. Nanotech. Lett. 3 (2011) 491–493.
[27] W. Wasel, K. Kuwana, P.T.A. Reilly, K. Saito, Carbon 45 (2007) 833–838.
[28] A. Botello-Méndez, et al., Chem. Phys. Lett. 453 (2008) 55–61.
[29] H. Ago, R. Ohdo, M. Tsuji, T. Ikuta, K. Takahashi, J. Nanosci. Nanotech. 10 (6) (2010) 3867–3872.
[30] S. Jeong, A. Oshiyama, Phys. Rev. Lett. 107 (2011) 065501 –1 – 06554.
[31] W.P. Wang, H.C. Wen, S.R. Jian, J.Y. Juang, Y.S. Lai, C.H. Tsai, W.F. Wu, K.T. Chen, C.P. Chou, App. Surf. Sc. 253 (2007) 9248–9253.
[32] W. Wang, R. Epur, P.N. Kumta, Electrochem. Commun. 13 (2011) 429–432.
[33] M. Alsawat, T. Altalhi, A. Santos, D. Losic, J. Phys. Chem. C. 121–25 (2017) 13634–13644.
[34] C. Mattevi, et al., J. Phys. Chem. C 112 (2008) 12207–12213.
[35] Y.J. Jung, B. Wei, R. Vajtai, P.M. Ajayan, Y. Homma, K. Prabhakaran, T. Ogino, Nano Lett. 3 (4) (2003) 561–564.
[36] J. Dijon, P.D. Szkutnik, A. Fournier, T. Goislard de Monsabert, H. Okuno, E. Quesnel, V. Muffato, E. De Vito, N. Bendiab, A. Bogner, N. Bernier, Carbon 48 (2010) 3953–3963.
[37] A. Barreiro, et al., J. Phys. Chem. B. 110 (2006) 20973–20977.
[38] O. Guellati, F. Antoni, M. Guerioune, D. Bégin, Catal. Today 301 (2018) 164–171.